Featured in Physics

# Cooperative Chain Dynamics of Tracer Chains in Highly Entangled Polyethylene Melts

M. Zamponi,[1] M. Kruteva,[2] M. Monkenbusch,[2] L. Willner,[2] A. Wischnewski,[2] I. Hoffmann,[3] and D. Richter[2]
[1]Forschungszentrum Jülich GmbH, Jülich Centre for Neutron Science at MLZ, Lichtenbergstraße 1, 85748 Garching, Germany
[2]Forschungszentrum Jülich GmbH, Jülich Centre for Neutron Science (JCNS-1) and Institute for Complex Systems (ICS-1), 52425 Jülich, Germany
[3]Institut Laue-Langevin (ILL), 71 Avenue des Martyrs, 38000 Grenoble, France

(Received 23 October 2020; accepted 12 March 2021; published 4 May 2021)

By neutron spin echo spectroscopy, we have studied the center of mass motion of short tracer chains on the molecular length scale within a highly entangled polymer matrix. The center of mass mean square displacements of the tracers independent of their molecular weight is subdiffusive at short times until it has reached the size of the tube $d$; then, a crossover to Fickian diffusion takes place. This observation cannot be understood within the tube model of reptation, but is rationalized as a result of important interchain couplings that lead to cooperative chain motion within the entanglement volume $\sim d^3$. Thus, the cooperative tracer chain motions are limited by the tube size $d$. If the center of mass displacement exceeds this size, uncorrelated Fickian diffusion takes over. Compared to the prediction of the Rouse model we observe a significantly reduced contribution of the tracer's internal modes to the spectra corroborating the finding of cooperative rather than Rouse dynamics within $d^3$.

DOI: 10.1103/PhysRevLett.126.187801

In the melt, long chain polymers interpenetrate strongly and entangle; the reptation model, a phenomenological approach, describes the resulting topological constraints by a virtual tube which follows the primitive path of a given test chain [1]. Chains slither along this tube thereby obeying the topological constraints. As an important further assumption, friction manifests itself only on the monomer level. Aside from the tube approach, theoretical concepts were brought forward with the aim of understanding the dynamics in long chain melts on a more fundamental level. In the mode coupling theory (MCT) approach of Schweizer [2], the tube ideas are replaced by strong nonlinear couplings between collective density fluctuations on the scale of the chain radius of gyration $R_g$. MCT leads to slowly fluctuating intermolecular forces that overcome the fast local dynamics rapidly [3]. The model predicts macroscopic transport coefficients, however, cannot properly depict the internal chain dynamics. Generalizing Schweizer's MCT approach, Guenza [4] considered a generalized Langevin equation (GLE), where, as a result of chain interpenetration, the chain motion is coupled within the range of their radius of gyration by a Gaussian interchain potential of mean force. Tube concepts compared to models involving collective dynamics differ essentially in the expectation for the dynamics of tracer chains in a strongly entangled matrix. As friction is a local phenomenon, within the tube approach, topological constraints do not affect tracer chains with a length in the order of an entanglement distance. As a result, free center of mass motion of the tracers has to be expected. On the other hand, interchain coupling causes cooperativity of chain motion also in the dynamics of short tracers. In this context, chain-chain interaction can no longer be lumped into a simple local friction. In consequence, cooperativity of motion is expected to affect short tracers, in particular, on short length scales, in the range of the interaction potential. The Rouse model treats the dynamics of a Gaussian chain in a heat bath [3]. There, the chain is subject to entropic forces and bead friction (monomeric friction coefficient $\xi_0$) giving rise to a center of mass diffusion $D_R = k_BT/(N\xi_0)$, where $N$ is the number of monomers, $k_B$ the Boltzmann constant, and $T$ the temperature. Some years ago, MD simulation in concert with neutron spin echo studies indicated subdiffusive behavior of the self-diffusion of short chains at times $t$ shorter than the longest intrachain relaxation time, the Rouse time $\tau_R = \xi_0 N^2 l_0^2/(3\pi^2 k_B T) \equiv 36 R_g^4/(\pi^2 W l_0^4)$, ($l_0$ the monomer length and the Rouse rate $W l_0^4 = 3 k_B T l_0^2/\xi_0$) [5,6]. Later on, these results were corroborated and augmented by Zamponi *et al.* [7] showing that, for short and weakly entangled chains, the short time subdiffusive mean square displacement (MSD) displays a crossover to Fickian diffusion at a decorrelation time of about $\tau_R$ of the respective chains. The phenomenon was interpreted in terms of Guenza's GLE approach [7,8]. The interchain coupling involves the lowest Rouse modes and the diffusion causing its subdiffusivity. Recently, Guenza [9] hypothesized that, in strongly entangled melts, cooperative chain fluctuations are restricted to the entanglement volume $\sim d^3$. Tracer diffusion, so far, was studied with macroscopic techniques, and an impressive set of asymptotic tracer diffusion results is available [10]. However, the initial regime with displacements in the range of the tube

 

diameter, the typical length scale imposed by the matrix polymer, is inaccessible by these techniques.

In this Letter, addressing this molecular length scale using neutron spin echo (NSE) spectroscopy, we present a systematic study of the MSD of short tracer chains with lengths in the range of an entanglement strand dispersed in a highly entangled host matrix focusing on the tracer chain. The following results stand out: (i) At short times independent of chain length, all tracer chains display subdiffusive center of mass motion $\langle r^2_{\rm com}(t)\rangle \sim t^{\beta}$ with $\beta \simeq 0.6, \ldots, 0.8$; (ii) when the center of mass MSD of the tracers has reached a critical value corresponding to the size of the tube confinement $\simeq d^2$, a crossover to Fickian diffusion $(D_{\rm tr} \sim N^{-1.85\pm0.05})$ is observed; (iii) compared to the Rouse prediction, the contributions of the tracer's internal motion are significantly reduced; (iv) these findings strongly support the hypothesis of cooperative chain motion within the entanglement volume $\sim d^3$ rather than individual Rouse-like chain relaxation as commonly supposed—an important feature that is missed by the reptation approach and revealed neither by MCT nor by GLE.

We studied the dynamic structure factors from labeled (hydrogenated) polyethylene (PE) tracer chains in a deuterated high molecular weight PE melt. Four different tracer molecular weights: 1.1, 2.15, 2.9, 4.16 kg/mol were investigated. The PE samples were obtained from anionically polymerized 1,4-polybutadiene and subsequent hydrogenation. The molecular weight of the long chain PE matrix was 40 kg/mol—a molecular weight, where within the accessible NSE time range tube-dissolving effects like contour length fluctuations and constraint release do not play a role [11]. It was prepared, accordingly, from fully deuterated 1,4-polybutadiene and subsequent deuteration. Each sample contained 5% protonated tracer molecules (2.9 kg/mol: 6%) in the deuterated PE matrix (for the molecular characteristics see Table I). The entanglement molecular weight $M_e \simeq 2.0$ kg/mol for PE is inferred from the tube diameter $d$ and was measured for long chain melts by NSE spectroscopy [11,12].

The experiments were performed using the IN15 spectrometer at Institut Laue-Langevin in Grenoble [13,14] at $T = 490$ K [15] spanning a time range $0.3\,\text{ns} \le t \le 500\,\text{ns}$ with a range of momentum transfers $0.03\ \text{Å}^{-1} \le q \le 0.08\ \text{Å}^{-1}$. The signal is dominated by the coherent single chain dynamic structure factor $S(q,t)/S(q,0)$ of the protonated tracer chains. However, at finite concentration, the structure factor of the long matrix chains with largely different dynamics also contributes to the observed spectra, in particular, adding a very slow component in the "plateau regime" at long times. The effect can be described and quantified in the framework of the dynamic random phase approximation (RPA) for polymer mixtures [16,17]. The computed ratio of model functions with and without this RPA contribution yields time-dependent correction factors. To exemplify, Fig. 1 displays the NSE spectra obtained from the PE1 sample together with the result of the dynamic RPA corrections. While the NSE spectra display a first decay that transforms into a plateau at long times, the dynamic RPA corrected spectra omit the plateauing and fall off continuously as is expected for a diffusing chain. The long time plateaus are a consequence of the RPA caused mixing of the dynamic structure factors from the short and long chains, the latter displaying the characteristic tube confinement restrictions at long times [11,12].

Thus, the corrected dynamic structure factors $S(q,t)$ allow us to extract $\langle r^2_{\rm com}(t)\rangle$ from

$$\frac{S(q,t)}{S(q,0)} = \exp\left(-\frac{q^2}{6}\langle r^2_{\rm com}(t)\rangle\right) f^{\rm int}_{\rm Rouse}(q,t), \qquad (1)$$

TABLE I. Molecular weight of the tracer polymers $M_n$, dispersity $Đ = M_w/M_n$, number of monomers $N$, Rouse diffusion coefficient $D_R$, tracer diffusion coefficients $D_{\rm tr}$ measured by NSE spectroscopy with an estimated statistical error of, at most, 2.0%.

| | $M_n$/kg/mol | Đ | $N$ | $D_R/\text{m}^2/s$ | $D^{\rm NSE}_{\rm tracer}/\text{m}^2/s$ |
|---|---|---|---|---|---|
| PE1 | 1.1 | 1.05 | 76 | $1.3\times10^{-10}$ | $1.07\times10^{-10}$ |
| PE2 | 2.15 | 1.05 | 147 | $6.5\times10^{-11}$ | $2.8\times10^{-11}$ |
| PE3 | 2.9 | 1.03 | 200 | $4.8\times10^{-11}$ | $1.6\times10^{-11}$ |
| PE4 | 4.16 | 1.02 | 285 | $3.3\times10^{-11}$ | $0.8\times10^{-11}$ |

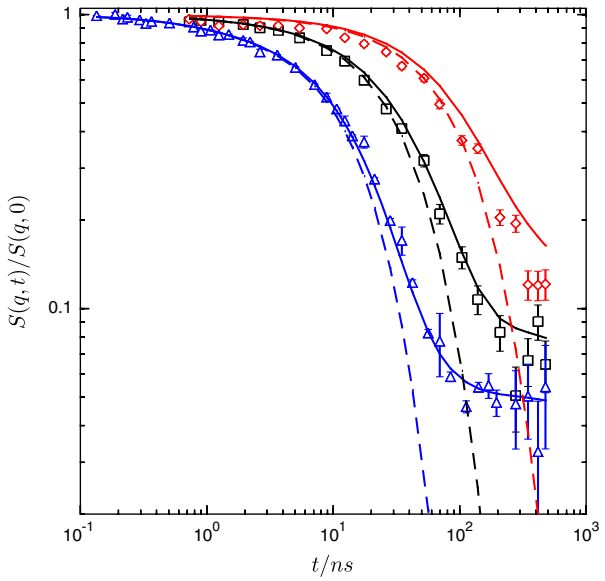


FIG. 1. Illustration of the dynamic RPA effect on the scattering function from the PE1 tracer chain at $q$ values from above: 0.03, 0.05, 0.08 Å$^{-1}$. The open symbols show the experimental NSE spectra, the solid colored lines the result of fitting with the dynamic RPA model, and dashed colored lines the RPA corrected scattering function. The results for 0.03 Å$^{-1}$ and for longer tracers turned out to be affected by too high instrument background and were omitted.

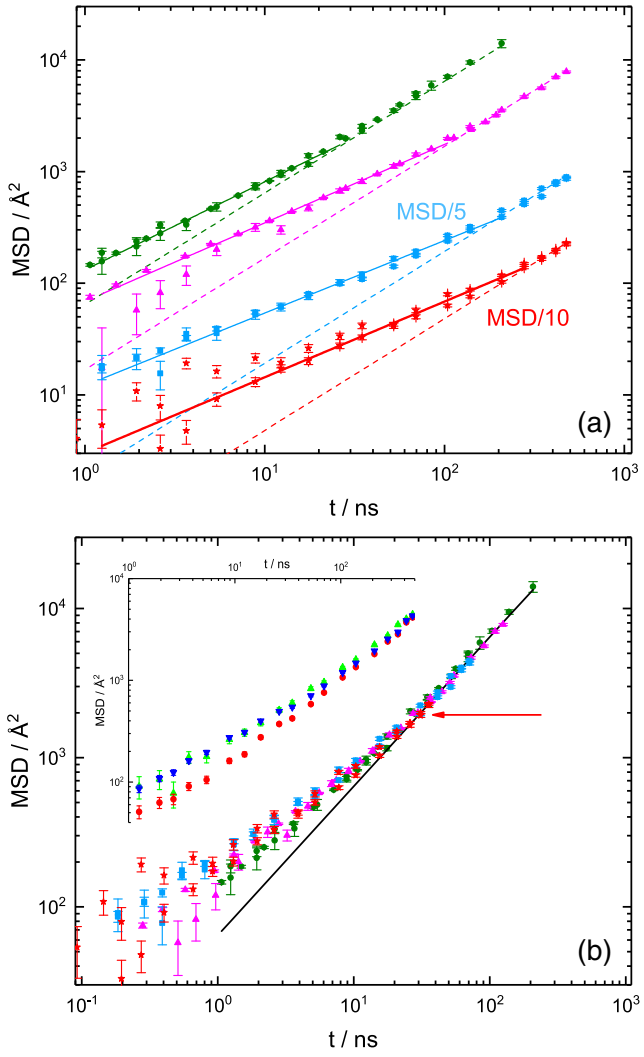


FIG. 2. (a) Center of mass mean square displacements MSD obtained from the RPA corrected NSE spectra. From above: PE1 (dots), PE2 (triangles), PE3 (squares), PE4 (stars); for better visibility the PE3 and PE4 MSD are shifted downwards by factors of 5 and 10, respectively. The dashed lines display the MSD due to Fickian diffusion, while the solid lines are fits to the subdiffusive regimes. (b) Master plot obtained by scaling the time axis by factors: PE1: 1.0; PE2: 0.26; PE3: 0.15; PE4: 0.075, symbols are the same as in part (a). The line indicates the Fickian diffusion law $\langle r^2_{\mathrm{com}}(t)\rangle \sim t$. The arrow marks the crossover MSD. The inset displays the MSDs obtained for PE3 from $q = 0.05$ Å$^{-1}$ (triangle) and from $q = 0.078$ Å$^{-1}$ with (dots) and without (reversed triangle) correction for the internal Rouse modes.

where $f^{\mathrm{int}}_{\mathrm{Rouse}}$ describes the contribution of the internal modes to $S(q,t)$ [18]. For $q = 0.03$ and $0.05$ Å$^{-1}$ $f^{\mathrm{int}}_{\mathrm{Rouse}} \simeq 1$, and an extraction of $\langle r^2_{\mathrm{com}}(t)\rangle$ is possible. With increasing $q$ and chain length, $f^{\mathrm{int}}_{\mathrm{Rouse}}$ is expected to contribute more significantly to the dynamic structure factor [see Fig. S4 in the Supplemental Material (SM) [19] ]. However, as it turns out, applying the Rouse correction as described in the SM [19] overcorrects the center of mass MSD. The inset in Fig. 2(b) compares the obtained MSD for the PE3 sample at $q = 0.05$ Å$^{-1}$ and $q = 0.078$ Å$^{-1}$ with and without applying corrections for the internal Rouse modes. From the inset in Fig. 2(b), it is quite clear that compensating for the expected internal mode contributions, at $q = 0.078$ Å$^{-1}$ overcorrects $\langle r^2_{\mathrm{com}}(t)\rangle$. The mode corrections at $q = 0.05$ Å$^{-1}$ are negligible, therefore, the congruence of the MSD derived from $q = 0.078$ Å$^{-1}$ without Rouse mode corrections with those from $q = 0.05$ Å$^{-1}$ is a strong indicator that the internal modes contribute much less than the Rouse model predicts. We conclude that the expected Rouse mode contribution to the spectra from the tracers does not materialize, and consequently, we evaluated the MSD without the Rouse correction. Figure 2(a) displays the NSE based MSD for the tracers of different chain length separately, revealing the results from the two different $q$ values taken into account. For all tracer chains, we observe a crossover from subdiffusive $\langle r^2_{\mathrm{com}}(t)\rangle \sim t^{\beta}$ at short times to $\langle r^2_{\mathrm{com}}(t)\rangle \sim t$ at longer times. In the subdiffusive regime, the time exponents amount to $\beta \simeq 0.6, \ldots, 0.8$ with $\beta$ decreasing for increasing $M_w$. In the linear time regime, the obtained MSDs perfectly coincide with the MSDs extrapolated from NMR (SM [19]) and scanning infrared microscopy (SIRM) [10] diffusion coefficients (Fig. 3). Thus, the observed crossover phenomenon is the transition from local subdiffusion to long range Fickian diffusion of the tracer.

Shifting the data horizontally with the ratio of diffusion coefficients onto one master curve [Fig. 2(b)] corroborates the phenomenon of a common crossover MSD for all tracers: The location of the MSD at crossover does not depend on the tracer chain length and is characterized by a critical $\mathrm{MSD}_{\mathrm{cr}}$ value. Fits of the $\mathrm{MSD}_{\mathrm{cr}}$ for the different tracers revealed PE1: $1970 \pm 100$ Å$^2$, PE2: $1975 \pm 100$ Å$^2$, PE3: $1900 \pm 100$ Å$^2$, and PE4: 1400 Å$^2$ (with a difficulty of specifying error; the Fickian diffusion regime is too short). This observation qualitatively differs from an earlier experiment on the self-diffusion in PE melts with molecular weights around the entanglement molecular weight $M_e$ [7]. There, also, a crossover from subdiffusivity at short times to a Fickian regime was observed. However, this crossover occurred around the respective Rouse times $\tau_R$ of the different chains with $\langle r^2_{\mathrm{com}}(\tau_R)\rangle \simeq R_g^2$ and could be well understood in terms of interchain coupling on the scale of the $R_g$. Since $R_g^2$ is proportional to $N$, there, the crossover MSD depends linearly on the chain length.

The present investigation yields MSD for all tracers with a crossover at about 2000 Å$^2$, independent of the tracer chain length. From NSE experiments, the tube diameter of the PE matrix had been determined to $d^2 = (47\ \text{Å})^2 = 2209$ Å$^2$ [11,12]. We note that tube dilution effects at low tracer concentrations are negligible [24]. Apparently, the crossover observed for the tracer MSD directly relates to the tube confinement exercised by the entangled matrix.

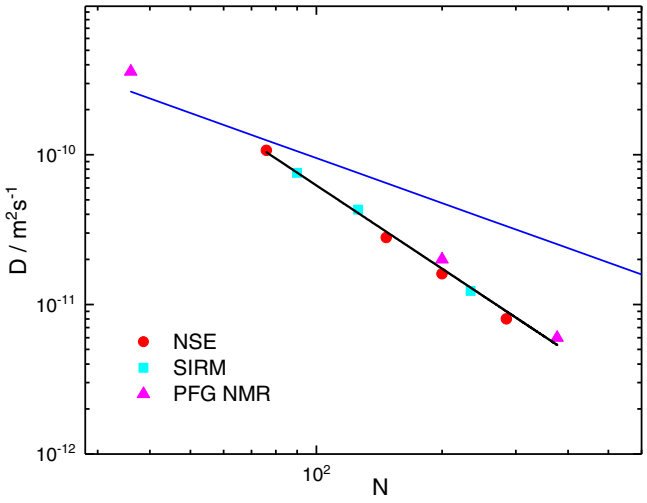


FIG. 3. Fickian diffusion coefficients at 490 K for different tracer chains as a function of number of monomers $N$: red dots: NSE; blue squares: scanning infrared microscopy [10]; pink triangles: PFG-NMR [19]. The interpolating black line marks a power law relationship: $D_{\mathrm{tr}} \sim N^{-1.85}$, the blue line shows the power law $D_{\mathrm{Rouse}} \sim N^{-1}$.

The long time diffusion coefficients are obtained from fitting $\langle r^2_{\mathrm{com}}(t)\rangle = 6D_{\mathrm{tr}}t$ in the linear time regime, where $\langle r^2_{\mathrm{com}}(t)\rangle \propto t$ (Table I). Together with macroscopic results, Fig. 3 displays the resulting $D_{\mathrm{tr}}$ as a function of molecular weight. Assuming no further intermediate diffusion regime, these limiting values should be consistent with the diffusion coefficients obtained by macroscopic methods. This is very well fulfilled. We include earlier SIRM results (squares) [10] as well as our pulsed field gradient (PFG) NMR results (triangles) (see SM [19]). Finally, the Rouse prediction $D_R$ (blue solid line) is also shown. Compared to the expectation from the Rouse model $D_R \propto N^{-1}$, the observed tracer diffusion is significantly slowed down, and its molecular weight dependence is much steeper than $N^{-1}$ and rather follows a slope $D_{\mathrm{tr}} \propto N^{-1.85\pm0.05}$. Other than for shorter chain melts, the apparent effective friction coefficient $\xi_0$ for tracer diffusion is determined by the long chain matrix and constant [25]. Therefore, all dependencies on tracer chain length are not related to different friction factors. For all tracer chains, we emphasize the good agreement between our microscopic and the macroscopic diffusion data both from PFG-NMR ($\mu$m scale) as well as from SIRM (mm scale). Apparently, the coupling mechanism leading to cooperative chain dynamics is also responsible for the observed strong $N$ dependence of the tracer diffusion coefficient (Fig. 3).

As the success of the packing model for entanglement formation suggests, entanglements appear to be a collective phenomenon involving a significant number of chains: As has been shown for a multitude of different polymer classes, for the formation of an entanglement in a polymer melt, about 20 uninterrupted chains need to pass through a given volume that, then, defines the entanglement volume $d^3$ [26]. This relationship was obtained by analyzing the connection between chain conformation, chain volume, and rheological response. Our results display the dynamic counterpart: within a volume spanned by the entanglement distance, chain motion is strongly coupled. It decorrelates for larger distances: After the tracer chain has moved by about one entanglement distance by center of mass diffusion, the interchain coupling is lifted, and the crossover to Fickian diffusion is observed. Since the entanglement distance is determined by the matrix, the crossover is observed at the same length scale independent of the tracer chain length. Thus, entanglements limit the range of cooperative dynamics, and the hypothesis of Guenza is corroborated [9]. We note, however, that, in Guenza's theory, the entanglement potential is not derived by a fundamental approach but has been added to the GLE heuristically. Schweizer's MCT approach relates to the correlation hole effect that takes place on the scale of $R_g$ and also does not reveal the entanglement scale.

The nature of friction is another important issue: As mentioned above, in the reptation concept, friction is strictly a local property establishing itself on the level of the polymer segment or monomer. Recent experimental results on local diffusion and internal relaxation of polyhedral oligomeric silsesquioxane (POSS) particles that consisted of a silica core with polyethylene oxide (PEO) oligomers attached to it, in a strongly entangled PEO matrix revealed a significant increase of the Rouse friction coefficient with the increase of the host molecular weight [27]. Evidently, the effective friction experienced by the probe particle that was significantly smaller than the entanglement distance in PEO (2 vs 5 nm), depends on how far the entanglement network is developed. We rationalize our observation of cooperative chain motion in the entanglement volume by suggesting that friction appears to be nonlocal on the scale of an entanglement.

As mentioned earlier, experimentally, evidence for chain coupling effects were observed on short chain melts with chains in the order of an entanglement length and below [4,6,7]. There, crossover effects to Fickian diffusion were found around a MSD $\approx R_g^2$ and $\tau_{\mathrm{cross}} \simeq \tau_R$ being consistent with MCT and GLE expectations. In contrast, short tracers acting as probes in a strongly entangled melt, even though with lengths below or slightly above the entanglement molecular weight, move cooperatively with the host chains to an extent limited by the tube size. Decorrelation is governed by the host: independent of tracer length, whenever the tracer MSD reaches a value comparable to the entanglement distance of the host, the tracer dynamics becomes uncorrelated, and the crossover to Fickian diffusion takes place. The observation tells us about the range of cooperative motion in a strongly entangled melt and appears as the dynamic counterpart to the packing model, where a critical volume spanned by about 20

interpenetrating chains leads to the formation of an entanglement. The observed cooperativity of chain dynamics within an entanglement volume also contradicts the common assumption of simple Rouse dynamics within the tube that, e.g., is a basis element in the interpretation of rheology results. As theoretical models on fundamental grounds predict a coupling range corresponding to $R_g$, the detailed coupling mechanism behind our observations will need further theoretical scrutiny.


[1] P. G. de Gennes, Reptation of a polymer chain in the presence of fixed obstacles, J. Chem. Phys. **55**, 572 (1971).

[2] K. S. Schweizer, Mode-coupling theory of the dynamics of polymer liquids: Qualitative predictions for flexible chain and ring melts, J. Chem. Phys. **91**, 5822 (1989).

[3] D. Richter, M. Monkenbusch, A. Arbe, and J. Colmenero, Neutron spin echo in polymer systems, Adv. Polym. Sci. **174**, 1 (2005).

[4] M. Guenza, Many chain correlated dynamics in polymer fluids, J. Chem. Phys. **110**, 7574 (1999).

[5] W. Paul, G. D. Smith, D. Y. Yoon, B. Farago, S. Rathgeber, A. Zirkel, L. Willner, and D. Richter, Chain Motion in an Unentangled Polyethylene Melt: A Critical Test of the Rouse Model by Molecular Dynamics Simulations and Neutron Spin Echo Spectroscopy, Phys. Rev. Lett. **80**, 2346 (1998).

[6] M. Guenza, Cooperative Dynamics in Unentangled Polymer Fluids, Phys. Rev. Lett. **88**, 025901 (2001).

[7] M. Zamponi, A. Wischnewski, M. Monkenbusch, L. Willner, D. Richter, B. Farago, and M. G. Guenza, Cooperative dynamics in homopolymer melts: A comparison of theoretical predictions with neutron spin echo experiments, J. Phys. Chem. B **112**, 16220 (2008).

[8] M. G. Guenza, Theoretical models for bridging timescales in polymer dynamics, J. Phys. Condens. Matter **20**, 033101 (2008).

[9] M. G. Guenza, Localization of chain dynamics in entangled polymer melts, Phys. Rev. E **89**, 052603 (2014).

[10] J. v. Seggern, S. Klotz, and H.-J. Cantow, Reptation and constraint release in linear polymer melts: an experimental study, Macromolecules **24**, 3300 (1991).

[11] A. Wischnewski, M. Monkenbusch, L. Willner, D. Richter, A. E. Likhtman, T. C. B. McLeish, and B. Farago, Molecular Observation of Contour-Length Fluctuations Limiting Topological Confinement in Polymer Melts, Phys. Rev. Lett. **88**, 058301 (2002).

[12] M. Zamponi, M. Monkenbusch, L. Willner, A. Wischnewski, B. Farago, and D. Richter, Contour length fluctuations in polymer melts: A direct molecular proof, Europhys. Lett. **72**, 1039 (2005).

[13] B. Farago, P. Falus, I. Hoffmann, M. Gradzielski, F. Thomas, and C. Gomez, The IN15 upgrade, Neutron News **26**, 15 (2015).

[14] M. Kruteva, B. Farago, I. Hoffmann, M. Monkenbusch, D. Richter, L. Willner, and M. Zamponi, Exploration and validation of random phase approximation (RPA) effects on the observed dynamical scattering from polymer mixtures, Institut Laue-Langevin (ILL), https://doi.ill.fr/10.5291/ILL-DATA.9-11-1947, 2020.

[15] Recalibrated by comparison with previous reference data.

[16] A. Z. Akcasu and M. Tombakoglu, Dynamics of copolymer and homopolymer mixtures in bulk and in solution via the random phase approximation, Macromolecules **23**, 607 (1990).

[17] M. Monkenbusch, M. Kruteva, M. Zamponi, L. Willner, I. Hoffmann, B. Farago, and D. Richter, A practical method to account for random phase approximation effects on the dynamic scattering of multi-component polymer systems, J. Chem. Phys. **152**, 054901 (2020).

[18] M. Doi and S. F. Edwards, *The Theory of Polymer Dynamics*, International Series of Monographs on Physics Vol. 73 (Oxford University Press, Oxford, 1994).

[19] See Supplemental Material at http://link.aps.org/supplemental/10.1103/PhysRevLett.126.187801 for more details on NMR measurements, Rouse mode contributions, and RPA corrections, which includes Refs. [20–23].

[20] E. O. Stejskal and J. E. Tanner, Spin diffusion measurements: Spin echoes in the presence of a time-dependent field gradient, J. Chem. Phys. **42**, 288 (1965).

[21] G. Fleischer and F. Fujara, NMR as a generalized incoherent scattering experiment, in *Solid State NMR I Methods* (Springer, Berlin, Heidelberg, 1994), pp. 159–207.

[22] P. E. Rouse, A theory of the linear viscoelastic properties of dilute solutions of coiling polymers, J. Chem. Phys. **21**, 1272 (1953).

[23] P. Schleger, B. Farago, C. Lartigue, A. Kollmar, and D. Richter, Clear Evidence of Reptation in Polyethylene from Neutron Spin-Echo Spectroscopy, Phys. Rev. Lett. **81**, 124 (1998).

[24] P. Malo de Molina, A. Alegría, J. Allgaier, M. Kruteva, I. Hoffmann, S. Prévost, M. Monkenbusch, D. Richter, A. Arbe, and J. Colmenero, Tube dilation in isofrictional polymer blends based on polyisoprene with different topologies: Combination of dielectric and rheological spectroscopy, pulsed-field-gradient NMR, and neutron spin echo (NSE) techniques, Macromolecules **53**, 5919 (2020).

[25] M. Zamponi, A. Wischnewski, M. Monkenbusch, L. Willner, D. Richter, A. E. Likhtman, G. Kali, and B. Farago, Molecular Observation of Constraint Release in Polymer Melts, Phys. Rev. Lett. **96**, 238302 (2006).

[26] L. J. Fetters, D. J. Lohse, D. Richter, T. A. Witten, and A. Zirkel, Connection between polymer molecular weight, density, chain dimensions, and melt viscoelastic properties, Macromolecules **27**, 4639 (1994).

[27] M. Lungova, M. Krutyeva, W. Pyckhout-Hintzen, A. Wischnewski, M. Monkenbusch, J. Allgaier, M. Ohl, M. Sharp, and D. Richter, Nanoscale Motion of Soft Nanoparticles in Unentangled and Entangled Polymer Matrices, Phys. Rev. Lett. **117**, 147803 (2016).